

Diagnostics and Prognostics of Wire-Bonded Power Semi-Conductor Modules subject to DC Power Cycling with Physically-Inspired Models and Particle Filter

Nicolas Degrenne, Stefan Mollov

Mitsubishi Electric R&D Centre Europe, 1 allée de Beaulieu, 35708 Rennes, France
n.degrenne@fr.mercede.mee.com
s.mollov@fr.mercede.mee.com

ABSTRACT

This paper presents an algorithm for determining the State of Health (SoH), the End of Life (EoL), and the Remaining Useful Life (RUL) of wire-bonded power semi-conductor modules. It is hybrid in two senses: a) it combines the estimations of physically-inspired models and the on-line data acquisition and b) it combines damage accumulation-based (i.e. stress counting) and condition-based (i.e. Von measure) prediction methods.

More precisely, the algorithm measures the die temperature and on-state voltage $V_{on,meas}$. A degradation model and an electrical models convert the temperature cycles into a estimation of the on-state voltage $V_{on,est}$. This estimation is confronted to $V_{on,meas}$ and the degradation model is corrected based on this confrontation. Thus, the degradation model is corrected on-line, which potentially allows to reduce the modeling and testing efforts necessary to generate an accurate degradation model.

A key aspect is the analysis, modeling, estimation, correction and exploitation of the on-state voltage V_{on} evolution. This paper presents a physically-inspired model that estimates V_{on} based on the damage estimated by the degradation model.

The algorithm is demonstrated with a particle filter and with power cycling experimental tests performed until complete wire-bond failure. The paper shows that the algorithm is capable of predicting the RUL with an accuracy of less than $\pm 10\%$ with a prognostic horizon of 50% of the lifetime.

1. INTRODUCTION

The internet of things applied to power semi-conductor modules would permit to communicate on-line condition (e.g. mission profile) and health (e.g. level of degradation of wire-bonds) for improved:

1. Availability

Nicolas Degrenne et al. This is an open-access article distributed under the terms of the Creative Commons Attribution 3.0 United States License, which permits unrestricted use, distribution, and reproduction in any medium, provided the original author and source are credited.

2. Security
3. Life-cycle cost
4. Reliability
5. Design

The on-state voltage V_{on} (at high current) is considered as a convenient parameter to monitor on-line because it applies generically to IGBT, MOSFETs and diodes (Bryant, 2017). V_{on} provides information on temperature, current, and degradation level (Degrenne et al., 2015). In case of wire-bonded power modules, a recognized damage sensitive parameter is the electrical resistance increase ΔR due to the degradation of the top-side connection (i.e. wire-bonds and metallization) (Ji et al., 2013) (Degrenne et al., 2015).

$$V_{on} = f(T_j, I_c, \Delta R) \quad (1)$$

Figure 1 presents a generic approach for health management of power semi-conductor modules. It is based on methods using V_{on} as a damage sensitive parameter.

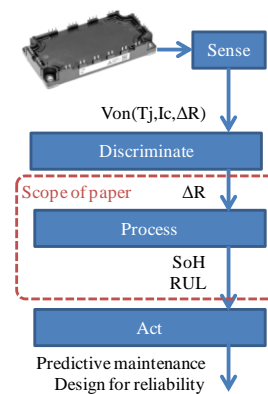


Figure 1 The scope of the paper is the processing step for generation of information (feature extraction and analysis)

V_{on} sensors were reviewed in 2013 in (Ghimire et al., 2013) and several works have been reported since then.

Techniques for discriminating temperature, current and degradation were reported (Eleffendi et al., 2015) (Singh et al. 2017) (Degrenne et al., 2018a), though research is still required to develop more accurate sensors and methods with a lower cost.

This paper deals with processing V_{on} data in order to extract useful information such as the State of Health (SoH) the End of Life (EoL) and the Remaining Useful Life (RUL). After this information is generated with a known degree of confidence, it can be communicated for action (i.e. health management) (Degrenne et al., 2015) which can consist in: Reliability enhancement (i.e. stress reduction/redistribution) in the case of redundant systems or predictive maintenance. The data processing step requires a multi-disciplinary approach to combine expert knowledge in the fields of power electronics, mechanical failure propagation, and signal processing. Almost all methods in the literature require models that can either be pre-defined or auto-learned (e.g. machine learning). Physics-based models are generally preferred because they offer a logical understanding of the results and can be modified to adapt to different power modules (Yang et al., 2013), though the literature is dominated by examples of (exponential) empirical models (Saha et al., 2011) (Celaya et al., 2011) (Dusmez et al., 2015) (Biglarbegian et al., 2018) such as (2):

$$\Delta R = \alpha(e^{\beta t} - 1) \quad (2)$$

An analysis of the evolution of V_{on} until the End of Life (EoL) is proposed in (Degrenne et al., 2018b). The present paper focuses on the evolution of V_{on} before the first wire-bond lift-off to extract information on the RUL (Fig. 2), with the purpose of prognostics with long horizon.

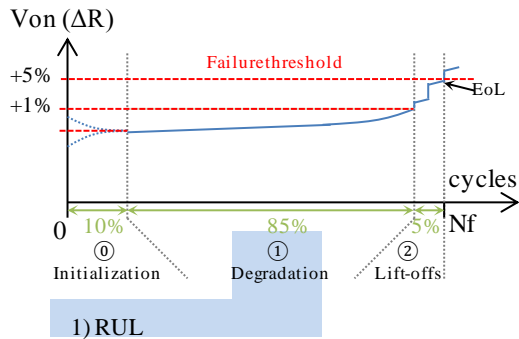


Figure 2 Generation of Remaining Useful Life (RUL) based on V_{on} analysis

After the first lift-off, phase ② represents only $\approx 5\%$ of the number of cycles to failure criteria (5% V_{on} increase). Thus, it could be considered, with no major error on the result, that the EoL is largely represented by the time of the 1st wire-bond lift-off for the purposes of RUL.

During the degradation phase ①, the thermo-mechanical stress provokes:

1. Reconstruction of the metallization
2. Crack propagation in wire-bonds

As illustrated in Fig. 2 and verified in Fig. 3, V_{on} increases in the range of 1-1.5% during the degradation phase ①. This increase was observed to be proportionately larger in other testing conditions.

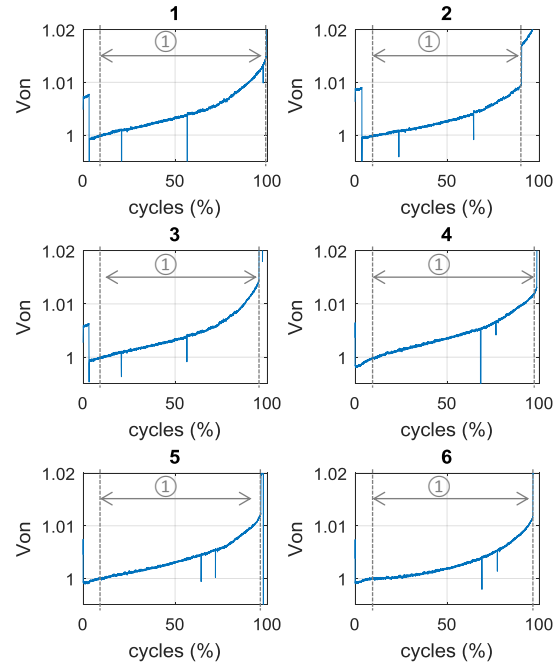


Figure 3 Normalized V_{on} evolution during power cycling for the 6 tested modules (zoom on degradation stage ①). The sudden voltage drops are measurement artifacts

First, the equipment for generating data and implementing the proposed RUL algorithm is presented. Then we explain the developed failure models. Next, the algorithm using a particle filter for RUL estimation is presented. Finally, prognostics results are presented and discussed.

2. EQUIPMENT AND METHODOLOGY

2.1. Device under test

In commercial IGBT power modules, wire-bonds are preferred top connections because of cost aspects. They are usually considered as the weakest connection that determines the end of life (Degrenne et al. 2015). In an effort to provide a representative example of the market, commercially available 1200V/150A wire-bonded IGBT module was selected as a DUTs (device under test). The module includes 3 half-bridge legs.

2.2. Power cycling at $\Delta T=70^\circ\text{C}$

Power cycling tests with reasonably low acceleration factor ($\Delta T=70^\circ\text{C}$, $T_{mean}=90^\circ\text{C}$) were realized with a custom test bench on the middle half-bridge. The high-side IGBT failed

first for all modules (5% V_{on} increase criteria corresponds to 100% cycles). Figure 4 shows a picture of its wire-bond pattern after failure. The metallization reflectivity is visibly reduced and the six long wire-bonds (1-6) are lifted-off.

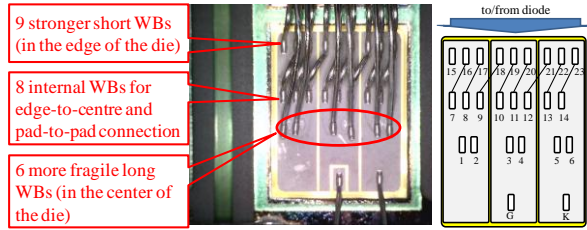


Figure 4 Wire-bond lay-out of the high-side IGBT picture (after power cycling, with gel removed) and schematic

The data of V_{on} evolution was measured by the voltage sensor of the test bench. The first 10% of the data are truncated because they correspond to a settling time where current is adjusted to provide the correct ΔT_j during the power cycling tests. In field condition, this settling time is not present and no data needs to be truncated.

The particular case of DC power cycling simplifies the models since the current and the associated stress during the measurement are considered constant.

2.3. General view of the estimation algorithm

A general view of the algorithm for RUL and EoL estimation is proposed in Fig. 5. The inputs to the procedure are the measured temperature history $T_{j,meas}(n-1..n)$ and the on-state voltage $V_{on,meas}(n)$ at moment n when the procedure is activated. The procedure is activated regularly every k thermal cycles. It first estimates the SoH. It then estimates the evolution of the SoH in the future (index m) in order to estimate the EoL and the RUL.

The algorithm counts the temperature cycles and uses a degradation model and an electrical model to estimate the on-state voltage $V_{on,est}(n)$ based on the measured junction temperature history $T_{j,meas}(n-1..n)$ between activations $n-1$ and n . $V_{on,est}(n)$ is combined with the measured value of on-state voltage $V_{on,meas}(n)$ in the re-sampling block to generate the SoH. The SoH consists of the corrected values of the resistivity increase of the metallization $R_{met,corr}(n)$, of the crack length increase $L_{crk,corr}(n)$, and of the on-state voltage $V_{on,corr}(n)$.

For SoH extrapolation at index $n+m$, the history of past temperature cycles $\Delta T_{j,meas}(0..n)$ is used to predict the next temperature cycles $\Delta T_{j,meas}(n+m-1..n+m)$. These temperature cycles are used as the inputs of the degradation and electrical models. The output is an estimation of the State of Health $SoH(n+m)$ at index $n+m$. The extrapolation is performed iteratively with increasing m until the SoH parameters cross a threshold value. This crossing point defines the EoL (index $n+m$) and the RUL (index m).

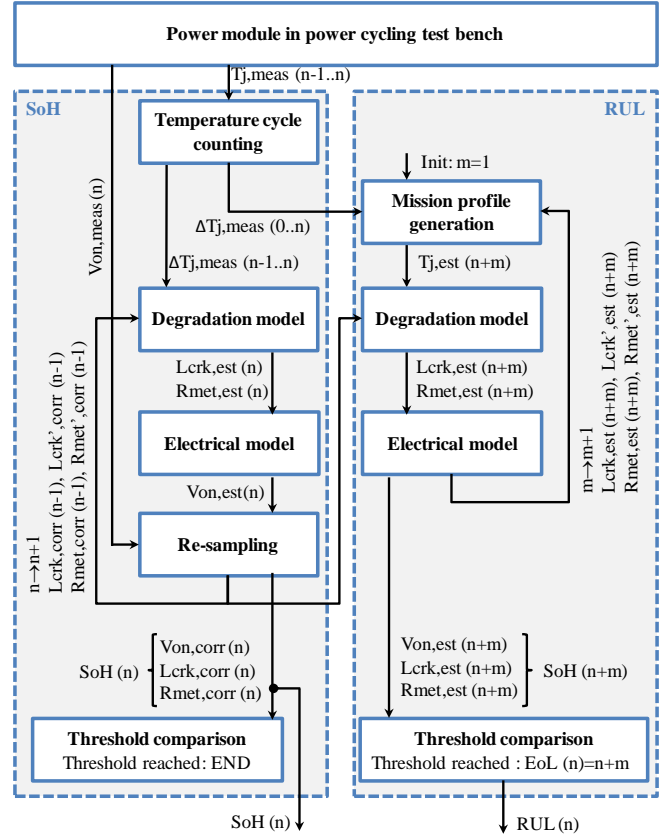


Figure 5 General view of the algorithm for SoH and RUL estimation

3. DEGRADATION MODEL

The objective of the degradation model is to estimate the crack length increase $L_{crk,est}(n)$ and the resistivity increase of the metallization $R_{met,est}(n)$ based on the temperature cycles between indexes $n-1$ and n and on the corrected crack length increase $L_{crk,corr}(n-1)$ and corrected resistivity increase of the metallization $R_{met,est}(n-1)$ at index $n-1$. The temperature cycles are estimated with a rainflow algorithm and are presented in the form of a histogram of temperature cycles. This algorithm is typically used for damage-accumulation based prediction of power modules (Mainka et al., 2011). In the case of RUL estimation, the temperature cycles at instant $n+m$ are extrapolated by the mission profile generation block. This block estimates the future temperature cycles $T_{j,est}(n+m)$ based on past temperature cycles $T_{j,meas}(1..n)$ and SoH at instant $m-1$.

3.1. General model for on-line implementation

The general implementation of the degradation model is described in Fig. 6. The damage law converts cycles of temperature into damage values (expressed in %). This law is either fitted to $Nf=f(\Delta T_j)$ curves provided by the manufacturer or established by a previous power cycling

4. ELECTRICAL MODEL

The objective of the electrical model is to convert the physical parameters $Lcrk,est(n)$ and $Rmet,est(n)$ into an estimation of the on-state voltage $Von,est(n)$.

4.1. Resistivity of metallization

The die Aluminum metallization is few micro-meters thick. Its role is to spread the current across the die cells and to offer an interface for wire-bonding. One consequence of its reconstruction is the increase of its resistivity during power cycling (Lutz et al., 2011). In this paper, we assume that a linear increase in the resistivity of the metallization leads to a linear increase in the resistance of the electrical connection. Thus, the on-state voltage at high current is related to the resistivity of the metallization with the following equation:

$$Von,met = \alpha + \beta \cdot Rmet, \quad (5)$$

where α and β are constants characteristic for each die type.

4.2. Cracks in wire-bonds

During power or passive cycling, crack propagation occurs near the joint interface (Lutz et al., 2011). Assuming unidirectional crack propagation L (Fig. 8), the joint area S is linearly reduced.

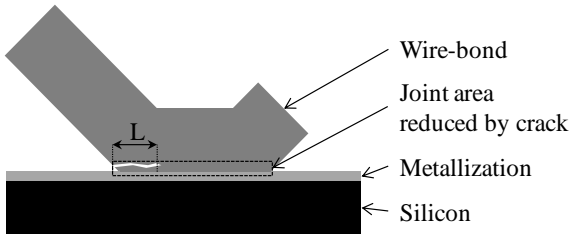


Figure 8 Crack length in the joint of a wire-bond

The resistance of a wire-bond subject to a linear crack length can therefore be expressed as (6):

$$R_{1WB} = \gamma + \frac{\delta}{1 - \varepsilon \cdot Lcrk_{1WB}} \quad (6)$$

where γ , δ and ε are constants depending on the stitch process.

This relation (6) is also valid to represent the equivalent resistance of an interconnection composed of multiple intact wire-bonds in parallel with a single wire-bond subject to a linear crack length of with several wire-bonds subject to a linear crack length at variable growth rate. The voltage drop across the wire-bonds in the degradation phase can therefore be expressed as (7):

$$Von,est = \gamma' + \frac{\delta'}{1 - \varepsilon' \cdot Lcrk,est} \quad (7)$$

where γ' , δ' and ε' are constants.

4.3. Overall electrical model

Finally, the overall on-state voltage Von is the sum of the voltage drops across the metallization and wire-bonds plus other voltage drops considered constant during the degradation phase:

1. Across the IGBT die (i.e. no degradation of the die, no dependence on T_j as implemented in (Degrenne et al., 2018a))
2. Across the low-side interconnection
3. Across the DBC tracks, lead-frames and external connectors

The combination of equations (5) and (7), plus other constant voltage drops, results in an overall physically-inspired model:

$$Von,est = a + b \cdot Rmet,est + \frac{c}{1 - d \cdot Lcrk,est} \quad (8)$$

where $a+c$ is the initial Von value, b defines the linear increase of Von caused by the linear resistivity increase of the metallization, and c and d define the increase caused by crack propagation in the wire-bond joints.

The parameters a , b , c and d were identified (curve fitting) during the degradation phase ① of the power cycling tests for each of the 6 DUTs. Boundary conditions for each parameter were defined to allow fast convergence. The experimental and modeled curves are presented in Fig. 9 and the alignment between the curves before the first bond lift off is very good indeed. Figure 9 therefore demonstrates the validity of equation (8) to describe the evolution of Von during the degradation phase ①.

4.4. Parameter Identification

Unlike the above validation and the prognostics method presented in (Degrenne et al., 2018b) where the parameters a , b , c and d are identified with curve fitting to the experimental measurements, the present algorithm uses the model (8) with parameters pre-defined based on the following analysis of typical on-state voltage curves as presented in Fig. 3.

Initially, when the power module is new ($n=0$), the normalized Von equals 1. Thus, equation (8) simplifies into:

$$Von(n=0) = a + c = 1 \quad (9)$$

Figure 10 shows the contributions of the metallization and of the wire-bonds at the EoL for the DUT 1. The normalized Von increase attributed to the metallization $Von,met(EoL)$ is approximately 0.75%, and the normalized Von increase attributed to the wire-bonds $Von,wb(EoL)$ is also

approximately 0.75%. These values are typical for the 6 DUTs.

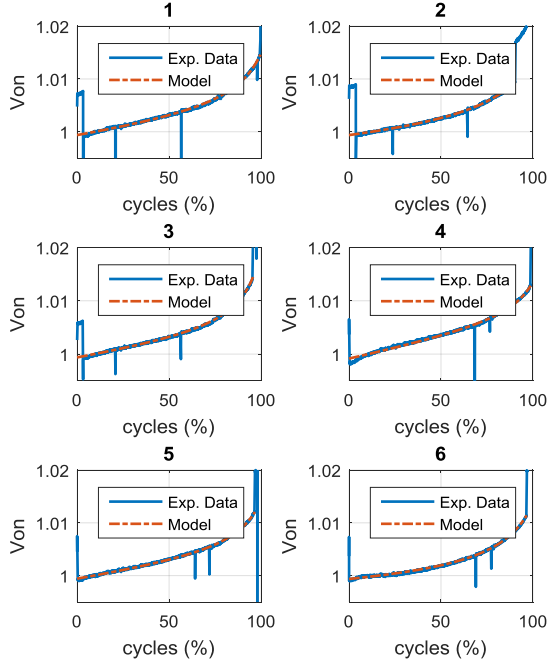


Figure 9 Comparison between V_{on} during power cycling and the model for the 6 tested modules.

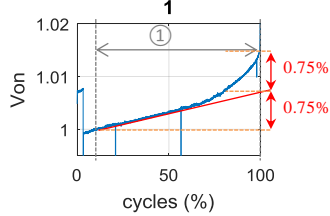


Figure 10 Contribution of the metallization (red curve, 0.75%) and of the wire-bonds 0.75% on the on-state voltage at the EoL for DUT 1.

At the EoL, the normalized increase in the resistivity of the metallization $R_{met}(EoL)$ and in the crack length $L_{crk}(EoL)$ are assumed to equal 1. This leads to the following equalities:

$$b = V_{on,met}(EoL) \quad (10)$$

$$\frac{c}{1-d} = V_{on,wb}(EoL) \quad (11)$$

In addition, the contribution of the wire-bond resistance at $n=0$ is considered to be one tenth of the one at the EoL. This ratio was found realistic after electrically modeling the wire-bonds.

$$c = \frac{V_{on,wb}(EoL)}{100} \quad (12)$$

Finally, these assumptions lead to the estimation of the parameters $a=0.99925$, $b=0.0075$, $c=0.000075$, and $d=0.99$.

The parameters of the electrical model are constant in the algorithm, and they are not corrected. The electrical model is considered exact and no error is added to its output.

5. RE-SAMPLING

The objective of the re-sampling block is to combine the estimated $V_{on,est}$ to the measured $V_{on,meas}$. More precisely, the likelihood of the particles of $V_{on,est}$ knowing $V_{on,meas}$ is used to decide whether the particle should be duplicated or not.

First, the probability density function of the measured on-state voltage $V_{on,meas}(n)$ is generated by adding the error $e2$ to the value measured by the sensor. The error $e2$ is assumed to have a normal distribution (e.g. domination of thermal noise) with a standard deviation of 0.1% (e.g. 2mV when $V_{on}=2V$). This is achievable in DC power cycling environment where the constraints (e.g. isolation, speed, cost) on the sensor are low, and where the measurement is performed at constant current and temperature.

$$V_{on,meas}(n) = V_{on,sensor}(n) + e2 \quad (13)$$

The measured and estimated particles of $V_{on,est}(n)$ and $V_{on,meas}(n)$ are compared one by one. For simplicity, the likelihood of the estimated value knowing the measured value is computed with the assumption of a normal distribution. The likelihood is expressed by:

$$Lkhd(n) = \frac{1}{\sigma\sqrt{2\pi}} \cdot \exp\left(\frac{-(V_{on,est}(n) - V_{on,meas}(n))^2}{2\sigma^2}\right) \quad (14)$$

where σ is the standard distribution arbitrarily set equal to the standard deviation on the measurement of V_{on} ($\sigma=0.1\%$).

In order to re-sample the particles based on the likelihood, the normalized cumulative sum of the likelihood is computed. As illustrated in Fig. 11, N_{part} numbers are randomly generated and compared to the cumulative sum in order to determine the particles that will be duplicated or removed.

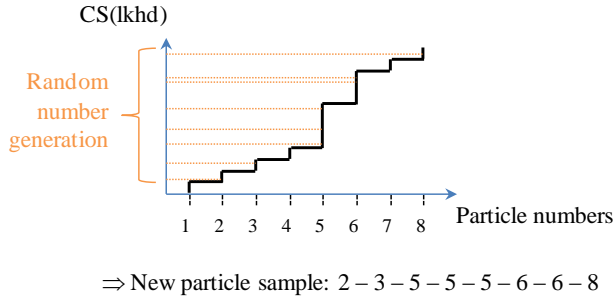


Figure 11 Illustration of the re-sampling method with an example with 8 particles

6. THRESHOLD COMPARISON

The SoH is compared with threshold values in order to detect the EoL and the RUL. The parameters $Lcrk,corr$ and $Rmet,corr$ are normalized such that their value should be 1 at the EoL. The associated threshold value is therefore 1. The parameter $Von,corr$ is normalized such that its value is 1 initially. The threshold is defined to equal 1.01 based on the experimental curves in Fig. 3. It was observed that power cycling with higher ΔT_j lead to higher threshold values. This increase of the threshold value was also observed to be larger in PWM power cycling tests where more heat is generated in the device due to switching losses.

7. RESULTS AND DISCUSSIONS

The algorithm was simulated using Matlab. It was activated $k=50$ times before EoL. The number of particles was set to $N_{part}=100$. These relatively low values were chosen to demonstrate that an intermittent and low processing effort is sufficient to accurately estimate the EoL and RUL.

The SoH and RUL estimated at each activation of the algorithm are plotted in Fig. 12. The initial predictions ($n=1$) correspond to the estimation predicted by the Coffin Manson model. When the algorithm is run (n increasing), the EoL estimates are corrected with measured $Von,meas$, and the EoL values estimated by $Rmet,corr$ and $Von,corr$ tend to converge towards to real value. Based on Fig. 12, it seems that $Rmet,corr$ and $Von,corr$ are the best parameters to follow for estimating the EoL and the RUL. On the contrary, $Lcrk,corr$ non-linearly impacts the on-state voltage mostly at the very end of life (equation (7)), and does not contribute to providing an early prognostics.

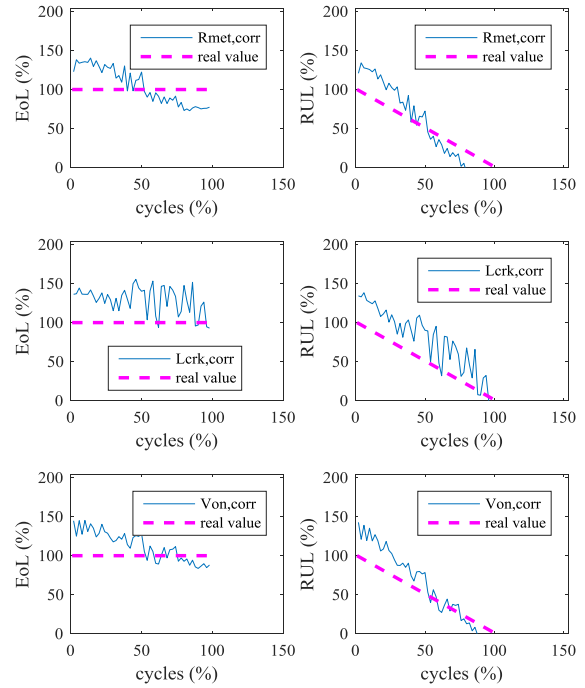


Figure 12 Mean estimation of the EoL and RUL as a function of number of cycle.

The detail of the SoH parameters for a long prognostic horizon (i.e. after 2% cycles only, $n=1$) is shown in Fig. 13. In this case, the extrapolation of the SoH states mainly relies on the initial values of the degradation and electrical models because only one correction was performed. The deviation observed on the EoL estimates is large because the errors propagate without correction. The particles which did not cross the threshold after 300% cycles are not represented in the histograms. Since the used optimistic Coffin Manson parameters tend to predict a higher EoL, the estimations after 2% cycles predict a higher EoL as well. The distributions of the estimates show that the error $e1$ of the degradation model is correctly estimated considering that the parameters of the Coffin-Manson model represent a worst case.

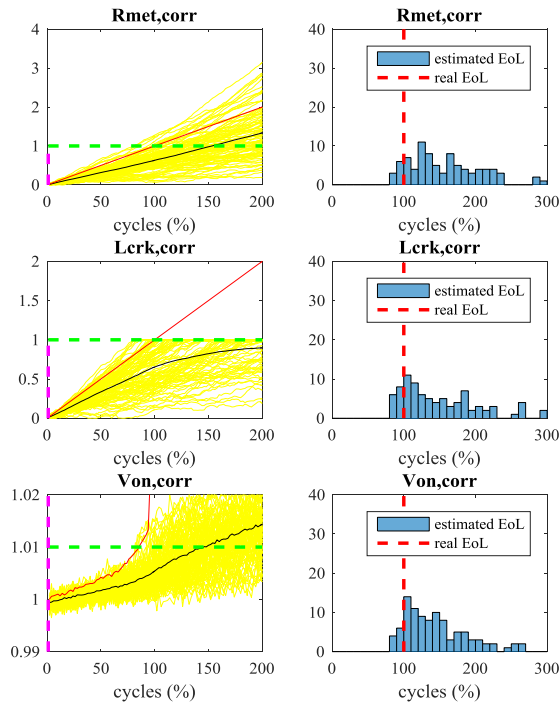


Figure 13 Details of the algorithm activated after 2% cycles. Identification and extrapolation of the SoH states (left) and corresponding EoL estimates (right). On the left, the particles and their mean are yellow and black, the real value is red, dashed curves show the activation time (magenta) and the threshold (green).

The detail of the SoH parameters for a medium prognostic horizon (i.e. after 50 cycles, $n=25$) is shown in Fig. 14. For *Rmet,corr* and *Von,corr*, the deviation on the EoL estimates is reduced. The average of the EoL estimates corresponds to the real EoL with a $\pm 10\%$ error.

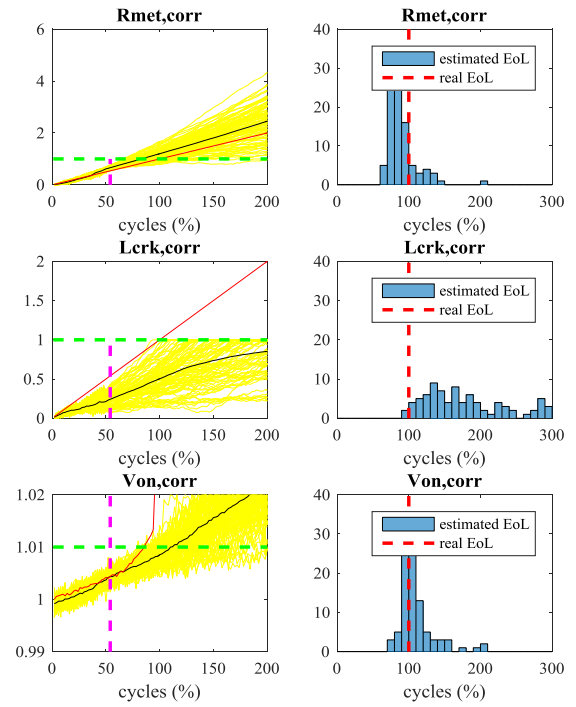


Figure 14 Details of the algorithm activated after 50% cycles. Identification and extrapolation of the SoH states (left) and corresponding EoL estimates (right). On the left, the particles and their mean are yellow and black, the real value is red, dashed curves show the activation time (magenta) and the threshold (green).

The detail of the SoH parameters for a shorter prognostic horizon (i.e. after 75% cycles) is shown in Fig. 15. The deviation on the EoL estimates is narrow (less than 20%), especially for *Rmet,corr* and *Von,corr*. The average EoL estimate based on these parameters slightly under-estimate the real EoL. This is because the real EoL is defined based on a 5% increase of Von (i.e. after several wire-bonds lifts-off), while the EoL estimated by the algorithm is defined as corresponding to the first wire-bond failure. This difference can be considered as a security margin.

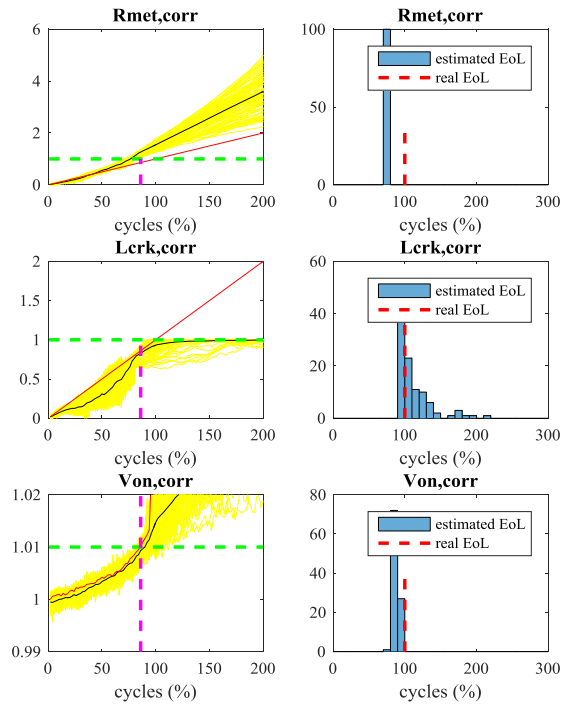


Figure 15 Details of the algorithm activated after 75% cycles. Identification and extrapolation of the SoH states (left) and corresponding EoL estimates (right). On the left, the particles and their mean are yellow and black, the real value is red, dashed curves show the activation time (magenta) and the threshold (green).

8. DISCUSSIONS AND PERSPECTIVES

The evolution of Von can thus be used not only for health assessment but also for RUL estimation. This has important implications since it would typically enable health management strategies such as predictive maintenance.

The algorithm demonstrated in this paper is a proof of concept that can be adapted and/or perfected in a number of ways. The major challenge is the adaptation to realistic mission profiles (as opposed to DC power cycling at constant ΔI). In the case of complex mission profiles, $Rmet$ and $Lcrk$ propagation rates are not a linear function of the number of cycles and the algorithm in Fig. 6 must be considered instead of the one in Fig. 7. Furthermore, several assumptions need to be revisited.

First, the degradation model relies on several strong assumptions used in the state-of-art (e.g. linear metallization resistivity ($Rmet$) and crack length ($Lcrk$) increase, Coffin-Manson model). Given the small amount of papers dealing with these physical phenomena, working on a stringent experimentally-validated physical degradation model is necessary.

Then, the electrical model also relies on strong assumptions (e.g. homogeneous current in metallization and wire-bonds, independence of temperature). The performance of finite element multi-physical modeling should help improve the electrical model.

Next, some parameters such as the error distributions and the threshold values were empirically or arbitrary defined without strong scientific justification. Their definition may influence the EoL estimation results and would require more investigation. In particular, PWM power cycling tests run in our lab indicate higher threshold values. It is therefore likely that a model generating the threshold value based on the measured temperature cycles will be necessary.

Finally, this algorithm relies on a Von measure/estimation with high precision/accuracy in the mV range, with low stability drift over the life time of the product, and without temperature or current dependency. This is achieved easily in accelerated ageing power cycling at constant ΔI with a measure performed at the beginning of the heating phase, but presents a challenge for on-line and at low-cost implementation for all power semiconductor devices of a converter switching at several kHz.

9. CONCLUSION

In next generation power modules, it is likely that data relative to condition and health will be monitored. Processing this data with physical knowledge allows generating the information in a comprehensive way with confidence. This paper demonstrates how it is possible to generate useful information based on Tj and Von sensors. Experimental validation is performed using power cycling data.

One outcome of the work is that the evolution of Von prior to first wire-bond lift-off can be used to estimate RUL with long prognostic horizon. One example illustrated by this work is by using the model with a particle filter for identification and extrapolation.

Future works will validate the algorithm in a more realistic PWM test bench operating with realistic mission profiles.

ACKNOWLEDGEMENT

The authors are thankful to Laurent Foube from Mitsubishi Electric R&D Centre Europe and to the anonymous reviewers for their constructive comments.

REFERENCES

- Biglarbegian, M., Mostafavi, S., Hauer, S., Nibir, S. J., Kim, N., Cox, R., & Parkhideh, B. (2018). On Condition Monitoring of High Frequency Power GaN Converters with Adaptive Prognostics. *In APEC 2018*.
- Bryant, A., (2017). Condition monitoring and junction temperature estimation: challenges of industrialisation. ECPE workshop on condition and health monitoring.

- Celaya, J., Saxena, A., Saha, S., & Goebel, kai F. (2011). Prognostics of Power MOSFETs under Thermal Stress Accelerated Aging using Data-Driven and Model-Based Methodologies. In *PHMC 2011*. Retrieved from http://www.phmsociety.org/sites/phmsociety.org/files/phm_submission/2011/phmc_11_009.pdf
- Degrenne, N., Ewanchuk, J., David, E., Boldyrjew, R., Mollov. (2015). A Review of Prognostics and Health Management for Power Semiconductor Modules. In *PHM society conference*.
- Degrenne, N., Mollov, S. (2018a). On-line Health Monitoring of Wire-Bonded IGBT Power Modules using On-State Voltage at Zero-Temperature-Coefficient. In *PCIM conference 2018*.
- Degrenne, N., Mollov, S. (2018b). Experimentally-Validated Models of On-State Voltage for Remaining Useful Life Estimation and Design for Reliability of Power Modules. In *CIPS conference 2018*.
- Dusmez, S., & Akin, B. (2015). Remaining Useful Lifetime Estimation For Degraded Power MOSFETs Under Cyclic Thermal Stress. In *ECCE 2015*. <http://doi.org/10.1109/ECCE.2015.7310203>
- Eleffendi, M. A., & Johnson, C. M. (2015). Evaluation of On-state Voltage VCE (ON) and Threshold Voltage Vth for Real-time Health Monitoring of IGBT Power Modules. In *EPE 2015*.
- Ghimire, P., Szymon, B., Munk-nielsen, S., Rannestad, B., & Bach, P. (2013). A review on real time physical measurement techniques and their attempt to predict wear-out status of IGBT. In *EPE 2013*.
- Ji, B., Pickert, V., Cao, W., & Zahawi, B. (2013). In situ diagnostics and prognostics of wire bonding faults in IGBT modules for electric vehicle drives. *IEEE Transactions on Power Electronics*, 28(12), 5568–5577. <http://doi.org/10.1109/TPEL.2013.2251358>
- Lutz, J., Schlangenotto, H., Scheuermann, U., & De Doncker, R. (2011). Semiconductor power devices: Physics, characteristics, reliability. *Berlin, Heidelberg: Springer Berlin Heidelberg*. <http://doi.org/10.1007/978-3-642-11125-9>
- Mainka, K., Thoben, M., Schilling, O. (2011). Counting Methods for Lifetime Calculation of Power Modules, Power-mag.com.
- Singh, A., Anurag, A., & Anand, S. (2017). Evaluation of Vce at Inflection Point for Monitoring Bond Wire Degradation in Discrete Packaged IGBTs. *IEEE Transactions on Power Electronics*. <http://doi.org/10.1109/TPEL.2016.2621757>
- Yang, L., Agyakwa, P. A., & Johnson, C. M. (2013). Physics-of-failure lifetime prediction models for wire bond interconnects in power electronic modules. *IEEE Transactions on Device and Materials Reliability*, 13(1), 9–17. <http://doi.org/10.1109/TDMR.2012.2235836>
- Yamada, Y., Takaku, Y., Yagi, Y., Nakagawa, I., Atsumi, T., Shirai, M., ... Ishida, K. (2007). Reliability of wire-bonding and solder joint for high temperature operation of power semiconductor device. *Microelectronics Reliability*, 47(12), 2147–2151. <http://doi.org/10.1016/j.microrel.2007.07.102>